

Preprint, Jun 21, 2018

Parallel solution, adaptivity, computational convergence, and open-source code of 2d and 3d pressurized phase-field fracture problems

Timo Heister *

Thomas Wick †

We present a scalable, parallel implementation of a solver for the solution of a phase-field model for quasi-static brittle fracture. The code is available as open source. Numerical solutions in 2d and 3d with adaptive mesh refinement show optimal scaling of the linear solver based on algebraic multigrid, and convergence of the phase-field model towards exact values of functionals of interests such as the crack opening displacement or the total crack volume. In contrast to uniform refinement, adaptive mesh refinement allows us to recover optimal convergence rates for the non-smooth solutions encountered in typical test problems. We also present numerical studies of the influence of the finite domain size on functional evaluations used to approximate the infinite domain.

Keywords: Phase-field fracture; parallel computing, scalability, influence of domain, deal.II

1 Introduction

In this work, we study the performance of the linear solver and the parallelization of our phase-field model for brittle fracture developed in [10] that allows 3d, adaptive solutions to more than 1024 cores and 100 million degrees of freedom. The original code was published on <https://github.com/tjhei/cracks> and is based on the Finite Element library deal.II [1]. While solver aspects for a similar problem have been discussed in [7], a scalable parallel implementation is novel.

We consider 2d and 3d benchmark problems in a pressurized fracture setting (Sneddon's tests [12]). While seemingly simple, it is a challenging test problem (that is prototypical for most phase-field fracture configurations) for the following reasons: First, the underlying energy functional is non-convex. Second, the reference problem is defined on an infinite domain, so approximation with a finite domain introduces errors. Third, due to the smeared interface zone, accurate representations of the total crack volume (TCV) and crack opening displacement (COD) requires a small phase-field regularization parameter and a very high resolution mesh around the crack region.

*Mathematical Sciences, Clemson University, Clemson, SC 29634, USA, heister@clemson.edu

†Institut für Angewandte Mathematik, Leibniz Universität Hannover, Welfengarten 1, 30167 Hannover, Germany, thomas.wick@ifam.uni-hannover.de

2 Notation and equations

Let $B \subset \mathbb{R}^d, d = 2, 3$ the total domain wherein $\mathcal{C} \subset \mathbb{R}^{d-1}$ denotes the fracture and $\Omega \subset \mathbb{R}^d$ is the unbroken domain. We assume homogeneous Dirichlet conditions on the outer boundary ∂B . Using a phase-field approach, the lower-dimensional fracture \mathcal{C} is approximated by $\Omega_F \subset B$ with the help of an elliptic (Ambrosio-Tortorelli) functional. For fracture formulations posed in a variational setting first proposed in [8], fracture regularizations using Ambrosio-Tortorelli functionals were developed in [4]. The unknown solution variables are vector-valued displacements $u : B \rightarrow \mathbb{R}^d$ and a smoothed scalar-valued indicator phase-field function $\varphi : B \rightarrow [0, 1]$. Here $\varphi = 0$ denotes the crack region and $\varphi = 1$ characterizes the unbroken material. The intermediate values constitute a smooth transition zone dependent on a regularization parameter ε . Adding a pressure $p : B \rightarrow \mathbb{R}$ that acts on the fracture boundary was first rigorously modeled and mathematically analyzed in [11]. Next, the physics require a crack irreversibility condition (the crack can never heal), which is an inequality condition in time, i.e, $\varphi \leq \varphi^{old}$, where φ^{old} denotes the previous time step solution. Consequently, modeling of fracture evolution problems leads to a variational inequality system, that is always, due to this constraint, quasi-stationary or time-dependent. Let $V := H_0^1(B), W := H^1(B)$ and $W_{in} := \{w \in H^1(B) | w \leq \varphi^{old} \leq 1 \text{ a.e. on } B\}$ be the function spaces to state the variational formulation. In the following, we denote the L^2 scalar product with (\cdot, \cdot) . The Euler-Lagrange system for pressurized phase-field fracture reads [10, 11]:

Formulation 1. *Let $p \in L^\infty(B)$ be given. For the loading steps $n = 1, 2, 3, \dots$: Find vector-valued displacements and a scalar-valued phase-field variable $\{u, \varphi\} := \{u^n, \varphi^n\} \in \{u_D + V\} \times W$ such that*

$$\left(((1 - \kappa)\tilde{\varphi}^2 + \kappa) \sigma(u), e(w) \right) + (\varphi^2 p, \operatorname{div} w) = 0, \quad (1)$$

$$(1 - \kappa)(\varphi \sigma(u) : e(u), \psi - \varphi) + 2(\varphi p \operatorname{div} u, \psi - \varphi) + G_c \left(-\frac{1}{\varepsilon}(1 - \varphi, \psi - \varphi) + \varepsilon(\nabla \varphi, \nabla(\psi - \varphi)) \right) \geq 0, \quad (2)$$

for all $w \in V$ and $\psi \in W_{in} \cap L^\infty(B)$. Here, G_c is the critical energy release rate, and we use the well-known law for the linear stress-strain relationship $\sigma := \sigma(u) = 2\mu_s e(u) + \lambda_s \operatorname{tr}(u)I$, where $\mu_s > 0$ and $\lambda_s > 0$ denote the Lamé coefficients, $e(u) = \frac{1}{2}(\nabla u + \nabla u^T)$ is the linearized strain tensor and I is the identity matrix, $\kappa > 0$. Finally, $\tilde{\varphi}$ is a linear extrapolation in time developed in [10] in order to convexify the above problem.

3 Solution algorithms and parallel framework

To solve Formulation 1, we employ a semi-smooth Newton method that was developed for phase-field fracture in [10] and combines two Newton methods: solving the nonlinear problem and treating the irreversibility constraint. The spatial discretization is based on a Galerkin finite element scheme, introducing H^1 conforming discrete spaces $V_h \subset V$ and $W_h \subset W$ consisting of bilinear/trilinear functions Q_1^c on quadrilaterals / hexahedra, respectively. The discretization parameter is denoted by h . The code is fully parallelized using MPI by building on the deal.II finite element library [1]. The adaptive meshes are handled by p4est [5] and the linear algebra is built on Trilinos [9]. This software framework is discussed in [2].

From our original work [10], we extended the active set strategy with a method to detect and constrain alternating active set indices to avoid cycles of the method similar to [6]. Additionally, we extended our refinement strategy from not only refining in the crack region to enforce $\varepsilon = 2h$ to also include a gradient jump estimator for the displacements. This is required to achieve rigorous computational convergence of the benchmark problem discussed here.

3.1 Linear iterative solution

The linear systems arising at each Newton step are solved iteratively using a GMRES scheme with a block diagonal preconditioner P^{-1} :

$$\begin{pmatrix} M_{uu} & 0 \\ M_{\varphi u} & M_{\varphi\varphi} \end{pmatrix} \begin{pmatrix} \delta u \\ \delta\varphi \end{pmatrix} = \begin{pmatrix} F_u \\ F_\varphi \end{pmatrix} \quad \text{with} \quad P^{-1} = \begin{pmatrix} \tilde{M}_{uu}^{-1} & 0 \\ 0 & \tilde{M}_{\varphi\varphi}^{-1} \end{pmatrix}.$$

Using the basis $\{\psi_i | i = 1, \dots, N\}$ in $V_h \times W_h$ with $\psi_i = (\chi_i^u, 0)^T, i = 1, \dots, N_u$ and $\psi_{N_u+i} = (0, \chi_i^\varphi)^T, i = 1, \dots, N_\varphi$ and $N = N_u + N_\varphi$, we have specifically the entries:

$$\begin{aligned} (M_{uu})_{i,j} &= \left(((1 - \kappa)\tilde{\varphi}^2 + \kappa) \sigma(\chi_j^u), e(\chi_i^u) \right) + (\sigma(\chi_j^u), e(\chi_i^u)), \\ (M_{\varphi u})_{i,j} &= 2(1 - \kappa)(\varphi \sigma(\chi_j^u) : e(u), \chi_i^\varphi) - 2(\alpha - 1)p(\varphi \operatorname{div}(\chi_j^u), \chi_i^\varphi), \\ (M_{\varphi\varphi})_{i,j} &= (1 - \kappa)(\sigma(u) : e(u)\chi_j^\varphi, \chi_i^\varphi) - 2(\alpha - 1)p(\operatorname{div}(u)\chi_j^\varphi, \chi_i^\varphi) + G_c \left(\frac{1}{\varepsilon}(\chi_j^\varphi, \chi_i^\varphi) + \varepsilon(\nabla\chi_j^\varphi, \nabla\chi_i^\varphi) \right). \end{aligned}$$

The block $M_{u\varphi}$ is zero due $\tilde{\varphi}$ in Equation (1).

We assume the existence of spectrally equivalent approximations \tilde{M}_{uu}^{-1} and $\tilde{M}_{\varphi\varphi}^{-1}$, which correspond to linear elasticity and a mixture of a Laplacian and mass matrix, respectively. The eigenvalues are given by the generalized eigenvalues of the systems $\tilde{M}_{kk} = \lambda M_{kk}$ ($k = u, \varphi$). We are approximating the blocks using a single V-cycle of algebraic multigrid (by Trilinos ML, [9]). Assuming the multigrid gives approximations independent of the mesh size h , the whole solver scheme is nearly optimal and independent of the number of processors and mesh size, as can be seen in Table 1.

ref	Dofs	NP							
		16	32	64	128	256	512	1024	2048
5	198'147	19	19	19	18	18	18	17	19
6	789'507	24	23	25	24	25	23	24	23
7	3'151'875	33	27	29	28	27	27	25	37
8	12'595'203	-	-	31	31	33	32	30	32
9	50'356'227	-	-	43	43	44	48	40	52

Table 1: Number of GMRES iterations of a single Newton step for the Sneddon 2d test with global refinement. Iterations are nearly independent of problem size (h) and number of processors NP . The relative residual is 1e-8.

Remark 1. *The parallelized linear solution of phase-field fracture was already implemented in [10] for 2d problems, but a computational analysis of the performance and the extension to 3d settings was missing up to now in the existing literature.*

4 Numerical tests: Sneddon 2d and 3d

We perform numerical tests in 2d and 3d. The benchmarks are based on the theoretical calculations of [12][Section 2.4 and Section 3.3]. A (constant) pressure $p = 10^{-3}Pa$ causes the fracture to change its width but not the length to form a penny-shaped crack. The initial crack of length $l_0 = 1.0$ is described with the help of the phase-field function φ . The domains are varied as $(-K, K)^d, d = 2, 3, K = 5, 10, 20, 40$ to approximate the infinite domain of the benchmark. We choose $G_c = 1$, Youngs' modulus as $E = 1$ and Poisson's ratio is $\nu = 0.2$. The regularization parameters are chosen as $\varepsilon = 2h$ and $\kappa = 10^{-12}h$. For more details of our computational configuration we refer the reader to [10][Section 5.3] (2d) and [13][Section 5.4] (3d).

We study the total crack volume (TCV) with analytical solutions from [12], respectively:

$$TCV_{h,\varepsilon} = \int_{\Omega} u \cdot \nabla \phi dx, \quad TCV_{2d} = \int_x 2u_y(x) dx = \frac{2\pi pl_0^2(1-\nu^2)}{E}, \quad TCV_{3d} = \int_x \int_y 2u_z(x,y) dx dy = \frac{16pl_0^3(1-\nu^2)}{3E} \quad (3)$$

where $l_0 = 1.0, E = 1.0, p = 1e-3, \nu = 0.2$. We note that the crack opening displacement (COD) is computed by

$$u_n(v) = \frac{cpl_0(1-\nu^2)}{E} \sqrt{1 - \left(\frac{\rho}{l_0}\right)^2}, \quad \text{with the radius } \rho = \|x\|_{l^2}, x \in R^d$$

with $n = y, v = x, c = 2$ in 2d and $n = z, v = (x, y), c = 4/\pi$ in 3d.

4.1 Convergence of total crack volume (TCV) in 2d

The first set of computations computes the error of the TCV in 2d for fixed values of ε while adaptively refining the solutions. Convergence for $h \rightarrow 0$ and $\varepsilon \rightarrow 0$ are clearly visible; see Fig. 1, left. This computation demonstrates: First, the phase-field regularization is a valid and convergent approximation of the fracture problem. Second, our approach for adaptive refinement is effective and the choice of $\varepsilon = 2h$ combined with adaptivity is a valid implementation strategy, that gives accurate solutions with a few number of unknowns.

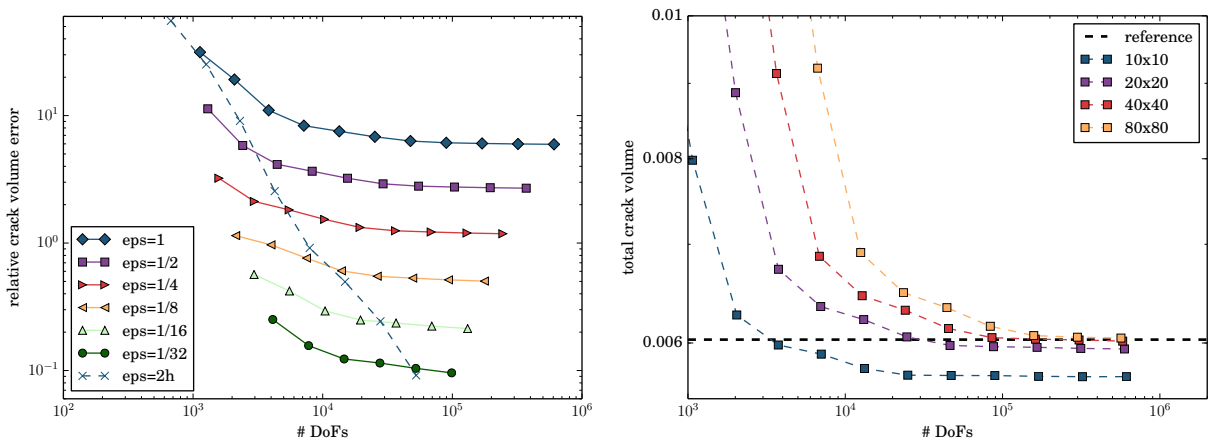


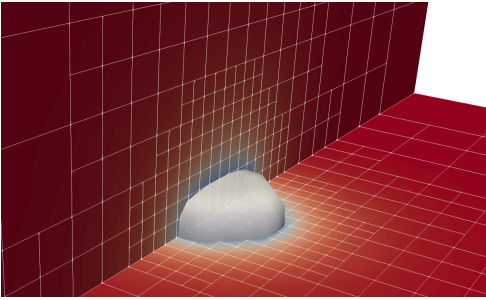
Figure 1: Left (Section 4.1): The convergence of ε on the 40x40 domain is computationally analyzed. Here we observe linear convergence in epsilon. Right (Section 4.2): dependence of functional value evaluations on the domain size.

4.2 Influence of finite domain size in 2d

The benchmark problem is stated for an infinite domain, so convergence is only obtained until this part of the error becomes dominant as can be seen in Fig. 1 (right). A larger size of the domain would raise the cost of the discretization immensely without adaptive mesh refinement, while we obtain more accurate solutions on a larger domain with about 10^5 unknowns and our refinement strategy. The extrapolated value of the TCV compared to the exact value of $6.0319\text{E-}03$ has an error of 5.6%, 1.5%, 0.5%, and 0.1% for the domain size of 10×10 , 20×20 , 40×40 , and 80×80 , respectively.

4.3 Convergence of the 3d benchmark

We now concentrate on the convergence of the TCV error for the 3d version of the same benchmark problem. Even with adaptive refinement, an accurate solution requires in the order of 100 million DoFs and substantial computing power (here run on 1024 cores); see Figure 2. On the one hand, this is a well-known challenge for smeared interface approaches. On the other hand, 3d computations for moving interface problems are still a challenge for ‘exact’ interface representations such as extended/generalized finite elements, cut cell methods, etc.. Therefore, these results show that phase-field approaches can give comparable results to other numerical methods.



ref	$10l_0/h$	# DoFs	eps	TCV	Error
4	16	12,436	2.1651E+00	3.5158E-02	586.67%
5	32	35,940	1.0825E+00	2.0078E-02	292.14%
6	64	105,740	5.4127E-01	1.0149E-02	98.22%
7	128	313,668	2.7063E-01	6.9110E-03	34.98%
8	256	946,852	1.3532E-01	5.8082E-03	13.44%
9	512	2,938,012	6.7658E-02	5.3764E-03	5.01%
10	1024	9,318,916	3.3829E-02	5.2131E-03	1.82%
11	2048	30,330,756	1.6915E-02	5.1567E-03	0.72%
12	4096	100,459,828	8.4573E-03	5.1352E-03	0.30%
reference (Sneddon)				5.1200E-03	

Figure 2: Section 4.3: Sneddon 3d adaptive convergence for a $10\times 10\times 10$ domain, $l_0 = 1$, using $\varepsilon = 2h$. Left: solution with mesh and isosurface for $\varphi = 0.3$. Right: convergence table.

4.4 Adaptive convergence of crack opening displacement (COD)

Finally, we study the crack opening displacement (COD) in 2d to compare adaptive vs. global refinement. For each domain size, the reference value is obtained using Richardson extrapolation of the numerical solution. As the solution is discontinuous, we see suboptimal convergence of the solution using global refinement, while we recover optimal rates using our adaptive scheme; see Figure 3.

Our results suggest a convergent method and lead us to expect an error estimate of the kind (similar to [14])

$$\begin{aligned} \|u_{h,\varepsilon} - u_{ref}\| &\leq \|u_{h,\varepsilon} - u_{ref,\varepsilon}\| + \|u_{ref,\varepsilon} - u_{ref}\| \\ &\leq C_1 \inf_v \|v - u_{ref,\varepsilon}\| + C_2 \varepsilon, \quad C_1, C_2 > 0, \end{aligned}$$

where the error of the discrete solution $u_{h,\varepsilon}$ to the exact solution u_{ref} is given by the sum of best-approximation error of the finite element method and an error term (i.e., a model error) introduced by the ε regularization converging linearly in ε .

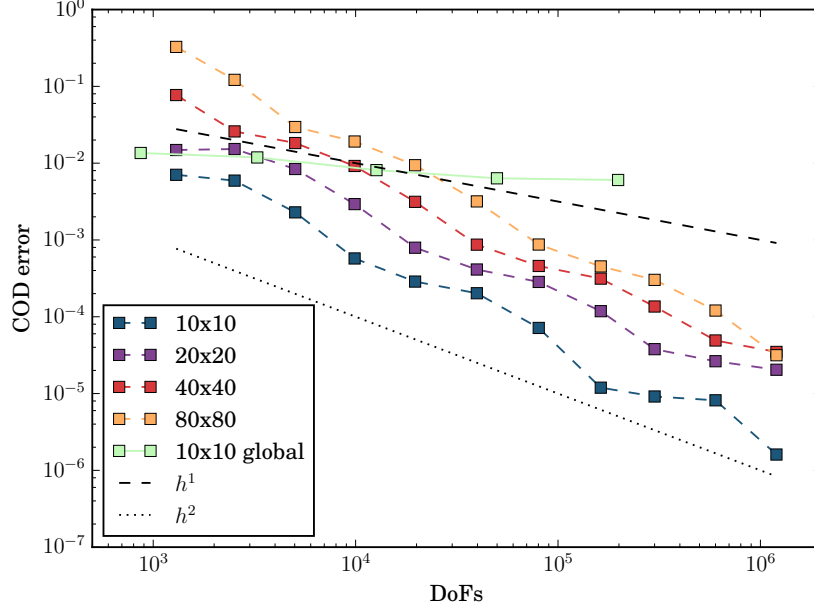


Figure 3: Section 4.4: Sneddon 2d error convergence to extrapolated COD values for a fixed domain size. We recover quadratic convergence in h using our adaptive refinement strategy. Errors are increasing for a fixed number of unknowns for a larger domain size, as the crack is resolved with fewer cells.

Acknowledgements

This work is supported by the German Priority Programme 1748 (DFG SPP 1748) Reliable Simulation Techniques in Solid Mechanics. Development of Non-standard Discretization Methods, Mechanical and Mathematical Analysis. Timo Heister was partially supported by the Computational Infrastructure in Geodynamics initiative (CIG), through the NSF under Award EAR-0949446 and The University of California Davis, by the NSF Award DMS-1522191, and by Technical Data Analysis, Inc through US Navy SBIR N16A-T003. Clemson University is acknowledged for generous allotment of compute time on Palmetto cluster.

References

- [1] D. Arndt, W. Bangerth, D. Davydov, T. Heister, L. Heltai, M. Kronbichler, M. Maier, J.-P. Pelteret, B. Turcksin, and D. Wells. *J. Numer. Math.*, **25**, 137–146 (2017).
- [2] W. Bangerth, C. Burstedde, T. Heister, and M. Kronbichler. *ACM Trans. Math. Softw.*, **38**, 14/1–28 (2011).
- [3] W. Bangerth, R. Hartmann, and G. Kanschat, *ACM Trans. Math. Softw.* **33**, 24/1–24/27 (2007).
- [4] B. Bourdin, G.A. Francfort, and J.-J. Marigo, *J. Mech. Phys. Solids* **48**, 797–826 (2000).
- [5] C. Burstedde, L. C. Wilcox, and O. Ghattas, *SIAM J. Sci. Comput.*, **33**, 1103–1133 (2011).
- [6] F. E. Curtis, Z. Han, D. P. Robinson, *Computational Optimization and Applications*, **60**, 311–341 (2015).
- [7] P. E. Farrell and C. Maurini, *Int. J. Numer. Meth. Engrg.*, **109**, 648–667 (2017).
- [8] G.A. Francfort and J.-J. Marigo, *J. Mech. Phys. Solids* **46**, 1319–1342 (1998).
- [9] M. Heroux, R. Bartlett, V. H. R. Hoekstra, J. Hu, T. Kolda, R. Lehoucq, K. Long, R. Pawlowski, E. Phipps, A. Salinger, H. Thornquist, R. Tuminaro, J. Willenbring, and A. Williams. *An Overview of Trilinos*, Technical Report SAND2003-2927 (2003).
- [10] T. Heister, M. F. Wheeler, and T. Wick, *Comp. Meth. Appl. Mech. Engrg.* **290**, 466 – 495 (2015).
- [11] A. Mikelić, M. Wheeler, and T. Wick, *ICES Report 14-18* (2014).
- [12] I. N. Sneddon and M. Lowengrub, *Crack problems in the classical theory of elasticity*, SIAM series in Applied Mathematics. John Wiley and Sons, Philadelphia, 1969.
- [13] M. F. Wheeler, T. Wick, W. Wollner, *Comp. Meth. Appl. Mech. Engrg.* **271**, 69–85 (2014).
- [14] T. Wick, *Comp. Mech.*, **57**(6), 1017–1035 (2016).